Extensive phosphorylation of AMPA receptors in neurons

Article *in* Proceedings of the National Academy of Sciences · August 2016

DOI: 10.1073/pnas.1610631113

5 authors, including:

Seok Heo
Johns Hopkins Medicine
22 PUBLICATIONS **129** CITATIONS
SEE PROFILE

Natasha K Hussain
Kavli Neuroscience Discovery Institute, John…
20 PUBLICATIONS **1,846** CITATIONS
SEE PROFILE

Bian Liu
Johns Hopkins University School of Medicine
11 PUBLICATIONS **92** CITATIONS
SEE PROFILE

Richard L Huganir
Johns Hopkins University
460 PUBLICATIONS **46,147** CITATIONS
SEE PROFILE

Extensive phosphorylation of AMPA receptors in neurons

Graham H. Diering[a,1], Seok Heo[a,1], Natasha K. Hussain[a,1], Bian Liu[a], and Richard L. Huganir[a,b,2]

[a]Solomon H. Snyder Department of Neuroscience, Johns Hopkins University School of Medicine, Baltimore, MD 21205; and [b]Kavli Neuroscience Discovery Institute, Johns Hopkins University, Baltimore, MD 21205

Contributed by Richard L. Huganir, July 1, 2016 (sent for review March 17, 2016; reviewed by Andres Barria and Katherine W. Roche)

Regulation of AMPA receptor (AMPAR) function is a fundamental mechanism controlling synaptic strength during long-term potentiation/depression and homeostatic scaling. AMPAR function and membrane trafficking is controlled by protein–protein interactions, as well as by posttranslational modifications. Phosphorylation of the GluA1 AMPAR subunit at S845 and S831 play especially important roles during synaptic plasticity. Recent controversy has emerged regarding the extent to which GluA1 phosphorylation may contribute to synaptic plasticity. Here we used a variety of methods to measure the population of phosphorylated GluA1-containing AMPARs in cultured primary neurons and mouse forebrain. Phosphorylated GluA1 represents large fractions from 12% to 50% of the total population under basal and stimulated conditions in vitro and in vivo. Furthermore, a large fraction of synapses are positive for phospho-GluA1–containing AMPARs. Our results support the large body of research indicating a prominent role of GluA1 phosphorylation in synaptic plasticity.

synaptic plasticity | excitatory synapse | AMPA receptor | protein kinase A | protein kinase C

Tetrameric AMPA-type glutamate receptors (AMPARs), made up from the subunits GluA1–4, mediate the majority of the fast excitatory synaptic transmission in the central nervous system (1). Regulation of AMPAR function is highly dynamic and represents a fundamental mechanism to control synaptic strength for many forms of synaptic plasticity, including long-term potentiation and depression (LTP/LTD) and homeostatic scaling (1).

The function and membrane trafficking of AMPARs is regulated by multiple interacting proteins, as well as by posttranslational modifications, including phosphorylation, palmitoylation, and ubiquitination (1). In particular, phosphorylation of GluA1 at S845 by cyclic-AMP–dependent protein kinase (PKA) (2) and at S831 by calcium/calmodulin-dependent protein kinase II (CaMKII) or protein kinase C (PKC) (3, 4) have been extensively studied. PKA-mediated phosphorylation of GluA1 S845 has been shown to promote GluA1 cell-surface insertion and synaptic retention, increase channel open-probability, facilitate the induction of LTP, and mediate homeostatic scaling-up, whereas dephosphorylation of S845 is associated with receptor endocytosis, LTD, and homeostatic scaling-down (5–13). CaMKII-mediated phosphorylation of GluA1 S831 increases channel conductance and regulates LTP (8, 13–16). Perhaps the strongest evidence for roles of GluA1 S845 and S831 phosphorylation comes from studies of mice with knockin mutations in which GluA1 phosphorylation is disrupted or mimicked. Several forms of behavior and synaptic plasticity in multiple brain regions require S845 or S831 phosphorylation, including hippocampal/cortical LTP and LTD, homeostatic plasticity, modulation of plasticity by neuromodulators, hippocampal spatial memory, fear-learning/extinction, appetitive incentive learning, and the action of antidepressants (8, 10–12, 17–23).

A recent study (24) used a variant of SDS/PAGE, called Phostag, to quantify the stoichiometry of GluA1 S845/S831 phosphorylation. Surprisingly, the authors of this study found that the levels of GluA1 phosphorylation were extremely low, even in synaptic fractions, contrary to earlier studies (9). This recent work reports that phospho-S831 and phospho-S845 GluA1 was less than 1% or 0.1% of total GluA1, respectively (24). These findings claimed to call into question the role of GluA1 phosphorylation in synaptic plasticity. Here we examined the extent of GluA1 phosphorylation using a variety of methods. Consistent with earlier work and models (1), we find that many of excitatory synapses are positive for phosphorylated GluA1, and a large fraction of the total GluA1-containing receptor population is phosphorylated. Approximately 15–20% of GluA1-containing AMPARs are phosphorylated at either S845 or S831 under basal conditions in vitro and in vivo, and these levels increase to ∼50% under certain pharmacological or behavioral stimulation conditions. We confirm the existence of GluA1-containing receptors dually phosphorylated at S845/S831. Thus, our findings support the important role of AMPAR phosphorylation in synaptic biology.

Results

Detection of Phospho-GluA1 Using Immunofluorescence Microscopy. First, we examined the distribution of phospho-GluA1–containing AMPARs at synapses using immunofluorescence microscopy. Rat hippocampal neurons were left untreated, or treated for 10 min with forskolin/rolipram (FR; 5 μM/100 nM) or phorbol-myristoyl-acetate (PMA; 1 μM) to selectively activate PKA or PKC, respectively, or the noradrenaline analog, isoproterenol (Iso; 5 μM), followed by fixation and immunolabeling using GluA1 and VGlut1 antibodies and phospho-specific antibodies

Significance

Decades of research from many laboratories has established a model in which phosphorylation of the GluA1 AMPA-type glutamate receptor subunit plays a significant role modulating long-term potentiation and depression, homeostatic and neuromodulator-regulated plasticity, spatial memory, fear/extinction, and appetitive incentive learning. However, a recent study suggests that GluA1 phosphorylation is exceedingly low, even in synaptic fractions. Here, we address this controversy using in vitro and in vivo techniques. We find a large fraction of excitatory synapses are positive for phosphorylated GluA1. Moreover, phosphorylated species make up a significant fraction of the population and are highly responsive to numerous physiologically relevant stimuli. This characterization reaffirms a large body of work defining a prominent role of AMPA receptor phosphorylation in synapse biology and synaptic plasticity.

Author contributions: G.H.D., S.H., N.K.H., and R.L.H. designed research; G.H.D., S.H., and N.K.H. performed research; G.H.D., S.H., N.K.H., and B.L. analyzed data; and G.H.D., S.H., N.K.H., B.L., and R.L.H. wrote the paper.

Reviewers: A.B., University of Washington; and K.W.R., National Institutes of Health, Receptor Biology Section/National Institute of Neurological Disorders and Stroke.

The authors declare no conflict of interest.

[1]G.H.D., S.H., and N.K.H. contributed equally to this work.

[2]To whom correspondence should be addressed. Email: rhuganir@jhmi.edu.

This article contains supporting information online at www.pnas.org/lookup/suppl/doi:10.1073/pnas.1610631113/-/DCSupplemental.

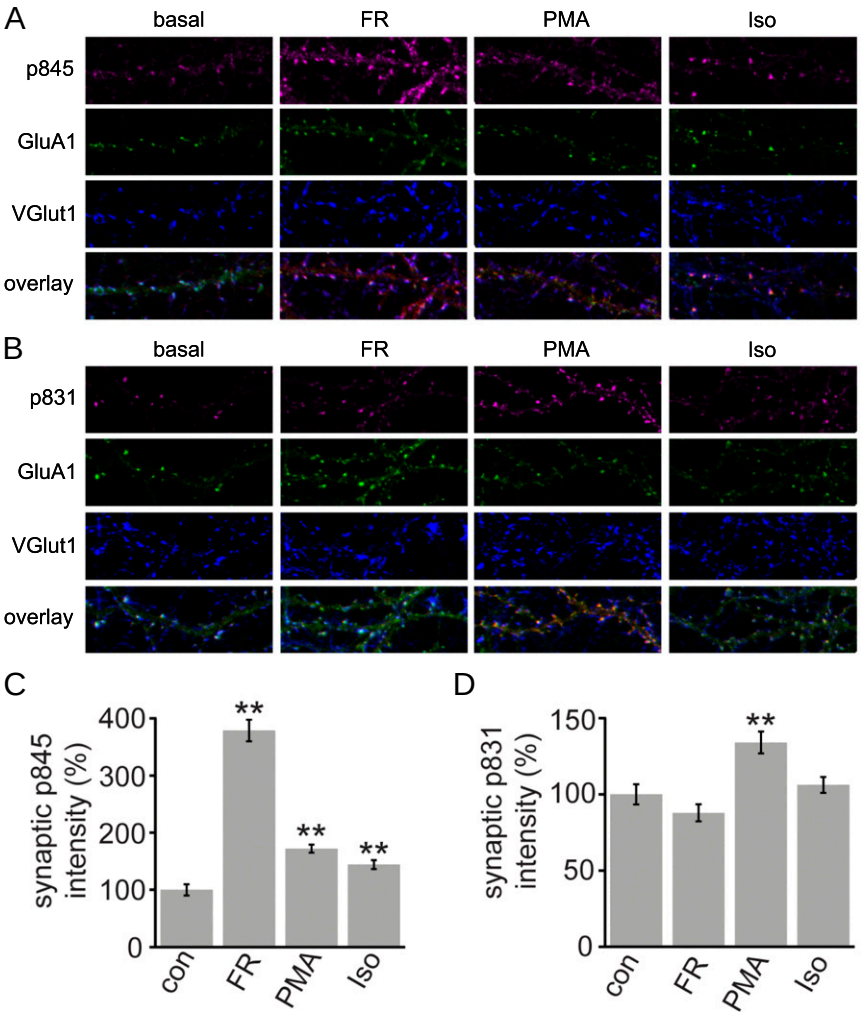

Fig. 1. Immunofluorescence detection of synaptic phospho-S845 and S831. (*A* and *B*) Rat hippocampal neurons (14 DIV) were treated with FR, PMA, or Iso for 10 min, followed by fixation and immunolabeling. Phospho-S845 (*A*) or phospho-S831 (*B*) shows clear punctate staining that overlaps with excitatory synapse marker VGlut1. Representative images are 40-μm dendritic segments. Quantification of phospho-S845 (*C*) or phospho-S831 (*D*) staining intensity at synapses. $^{**}P < 0.001$ (ANOVA followed by Fisher's PLSD post hoc test, $n = 20$–22 cells per group). Error bars indicate mean ± SEM. See also Figs. S1 and S2.

for S831 or S845 (Fig. 1). Synaptic phospho-GluA1 signal was identified as phospho-S845 or -S831 puncta overlapping with both VGlut1 and total GluA1. Under basal conditions, both antiphospho-S845 and -S831 showed punctate staining that overlapped with total GluA1 and the excitatory synapse marker VGlut1 (Fig. 1 *A* and *B*). Treatment with FR significantly increased the synaptic staining intensity of phospho-S845 (Fig. 1 *A* and *C*), whereas PMA treatment significantly increased the synaptic intensity of phospho-S831 (Fig. 1 *B* and *D*) [$^{**}P < 0.001$, ANOVA followed by Fisher's partial least-squares difference (PLSD) post hoc test, $n = 20$–22 cells per group]. Under basal conditions, 16% and 76% (SEM ± 3%, $n \geq 17$ neuronal fields for each condition) of synapses were positive for phospho-S845 and phospho-S831, respectively. FR or PMA treatment increased the percentage to 87% and 85% (SEM ± 3%, $n \geq 17$ neuronal fields for each condition), respectively. To validate the specificity of the phospho-GluA1 antibodies, we repeated our treatment and staining procedure using mouse cortical neurons cultured from WT or GluA1 phosphorylation site mutant (S845A or S831A) knockin mice (Fig. S1). FR treatment clearly increased the phospho-S845 staining intensity in WT or S831A neurons, whereas PMA treatment increased the staining intensity of phospho-S831 in WT and S845A neurons. However, no specific staining was seen with antiphospho-S845 in S845A neurons or with antiphospho-S831 in S831A neurons under any treatment conditions, confirming the specificity of these antibodies for immunolabeling (Fig. S1). In addition, with this immunolabeling method, we conclude that phosphorylation of S845 and S831 can occur independently, as mutation of one site did not prevent up-regulation of the other site under the appropriate stimulation conditions (Fig. S1). To further demonstrate the specificity of our immunolabeling, we treated fixed rat hippocampal neurons with alkaline phosphatase (CIP) before immunostaining (Fig. S2). We determined that phosphatase treatment significantly reduced phospho-S845 and phospho-S831 under basal as well as stimulated conditions ($P < 0.0001$ non-CIP vs. CIP-treated conditions, ANOVA; $n \geq 17$ neuronal fields for each condition). In summary, we found that a large fraction of synapses were positive for phospho-GluA1 species under basal and stimulated conditions and that the level of phospho-GluA1 content at synapses increases with stimulation.

Quantification of Phospho-GluA1 Containing AMPAR Tetramers Using Immunodepletion. In addition to showing specificity for immunostaining, we found that the antiphospho-S845 and -S831 antibodies quantitatively immunoprecipitated phospho-GluA1 (Fig. 2). We therefore examined the fraction of GluA1-containing AMPARs that were phosphorylated using an immunodepletion

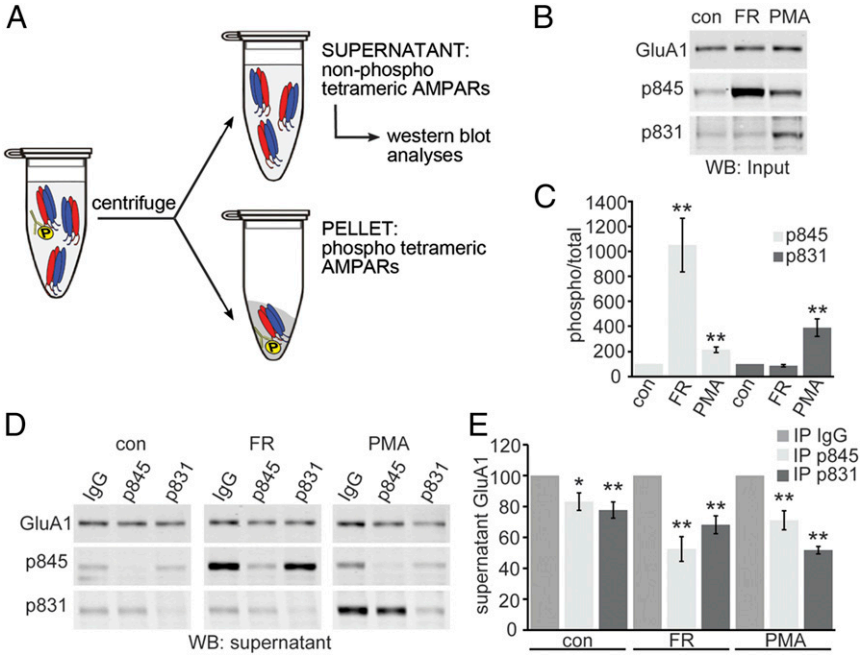

Fig. 2. Quantification of phospho-GluA1 containing tetramers by immunoprecipitation. (*A*) Schematic immunoprecipitation of phosphorylated GluA1-containing tetramers. Phospho-GluA1 accumulates in the pellet and is depleted from the supernatant, leaving unphosphorylated GluA1 in the supernatant. (*B*–*E*) Rat cortical neurons (13–14 DIV) were treated with FR or PMA for 10 min before lysis. (*B*) Western blot and (*C*) quantification of relative phospho-S845 and phospho-S831. (*D*) Control and FR/PMA treated neuronal lysates were subjected to immunodepletion using phospho-S845 or phospho-S831 antibodies. (*E*) Quantification of GluA1 remaining in the supernatant following immunodepletion with phospho-specific antibodies normalized to control depletion with IgG. Total and phosphorylated GluA1 were detected by Western blot simultaneously using a LiCor fluorescence scanner. $n = 5$. $^{*}P < 0.05$ and $^{**}P < 0.01$ indicate significant difference from IgG control. Error bars indicate mean ± SEM. See also Figs. S4 and S5.

assay with the phosphospecific antibodies. Rat cortical neurons were treated with or without FR or PMA for 10 min, followed by lysis and Western blot. The lysis condition retains AMPARs as tetramers (Fig. 2*A*) (25). FR treatment significantly increased levels of phospho-S845 and, to a lesser extent, phospho-S831, whereas PMA treatment significantly increased the levels of phospho-S831 (Fig. 2 *B* and *C*). Neuronal lysates were incubated overnight with control IgG or antiphospho-S845 or -S831 and protein A Sepharose beads. Phosphorylated GluA1 species are collected in the pellet following immunoprecipitation, whereas the nonphosphorylated GluA1 remains in the supernatant (Fig. 2*A*). Total and phospho-GluA1 content in the supernatant (unbound fraction) was then analyzed using quantitative Western blot (Fig. 2 *D* and *E*). Phospho-S845 and phospho-S831 receptors were immunodepleted by 80–90% by their respective antibodies (Fig. 2*D*). Furthermore, we determined that immunodepletion of neuronal lysates with antiphospho-S845/S831 also reduced total GluA1 signal relative to IgG control. This reduction of total GluA1 detected in the supernatants was quantified and represents the population of phosphorylated receptors depleted by immunoprecipitation. Using this assay we determined that under basal conditions, 16.8% and 22.3% of GluA1-containing AMPARs contain a phosphorylation at S845 or S831, respectively (Fig. 2 *D* and *E*). FR or PMA treatment, respectively, increased the amount of phospho-S845 or phospho-S831 GluA1-containing AMPARs to ∼50% (Fig. 2 *D* and *E*). Next, we examined the content of the immunoprecipitated fraction (pellet). Under FR or PMA treatment conditions, we find that phospho-S831 can be detected in the immunoprecipitate with antiphospho-S845 antibody and vice versa, indicating that under certain conditions, GluA1 containing AMPARs are phosphorylated on both S845 and S831 (Fig. S3*E*).

To test for the phospho-specificity of the immunoprecipitation, rat cortical neurons were treated with FR or PMA for 10 min before lysis. The lysates were then divided in half and treated with or without CIP to remove all phosphorylation, followed by immunoprecipitation with antiphospho-S845 or -S831 antibodies. We find that CIP treatment completely eliminates detection of phospho-GluA1 by the antiphospho-S845 and -S831 antibodies by Western blot, whereas detection of total GluA1 protein is unaffected (Fig. S3*A*). Furthermore, GluA1 is detected following immunoprecipitation with antiphospho-S845/S831 antibodies in control lysates but not in CIP-treated lysates or following immunoprecipitation with control IgG (Fig. S3*B*). To further confirm the specificity of antiphospho-GluA1 antibodies, we performed immunoprecipitation in mouse cortical neurons cultured from WT or phospho-mutant knockin mice. Antiphospho-S845 was able to immunoprecipitate GluA1 only in WT and S831A neurons, whereas antiphospho-S831 was able to immunoprecipitate GluA1 only in WT and S845A neurons (Fig. S3 *C* and *D*). These experiments confirm that antiphospho-GluA1 antibodies are able to immunoprecipitate GluA1 in a phospho-specific manner.

We repeated our immunodepletion experiments under maximal denaturation conditions in which AMPAR tetramers become dissociated into monomers (Fig. S4*A*) (25). Under basal conditions, phospho-S845 and -S831 make up 10.8% and 6.3% of the total GluA1 population, respectively. As expected, FR treatment increased the population of phospho-S845 receptors to 53.1%, whereas PMA treatment increased the population of phospho-S831 receptors to 29.6% (Fig. S4 *B* and *C*). Again we find that phospho-S831 is detected in the pellet following immunoprecipitation with antiphospho-S845 and vice versa, indicating the presence of dually phosphorylated S831/S845 GluA1 monomers (Fig. S4*D*).

We also wished to test whether changes in the population of phospho-GluA1–containing AMPARs could be detected under more physiologically relevant stimulation conditions. Rat cortical neurons were treated with NMDA or glycine, chemical stimuli

shown to induce LTD or LTP, respectively (cLTD/cLTP), and which are known to regulate S845 phosphorylation (26–28). Alternatively, neurons were treated with Iso, a noradrenaline analog known to result in phosphorylation of GluA1 S845 via activation of β-adrenergic receptors and PKA (10, 17, 23, 29, 30). cLTD treatment significantly reduced the levels of phospho-S845, whereas cLTP and Iso increased the signal of phospho-S845 (Fig. 3 *A* and *B*). Using our immunodepletion assay, we again find that under basal conditions, phospho-S845–containing receptors constitute ∼20% of GluA1-containing AMPARs. Iso and cLTP increased this population to 30–40% (Fig. 3 *C*–*F*), whereas cLTD decreased the number of phospho-S845 GluA1-containing AMPARs to 12.8% (Fig. 3 *G* and *H*). These results show that phospho-GluA1–containing receptors make up a significant fraction of the total receptor population, and that this phospho-population is regulated under plasticity conditions, in agreement with earlier work (9, 17, 31–34).

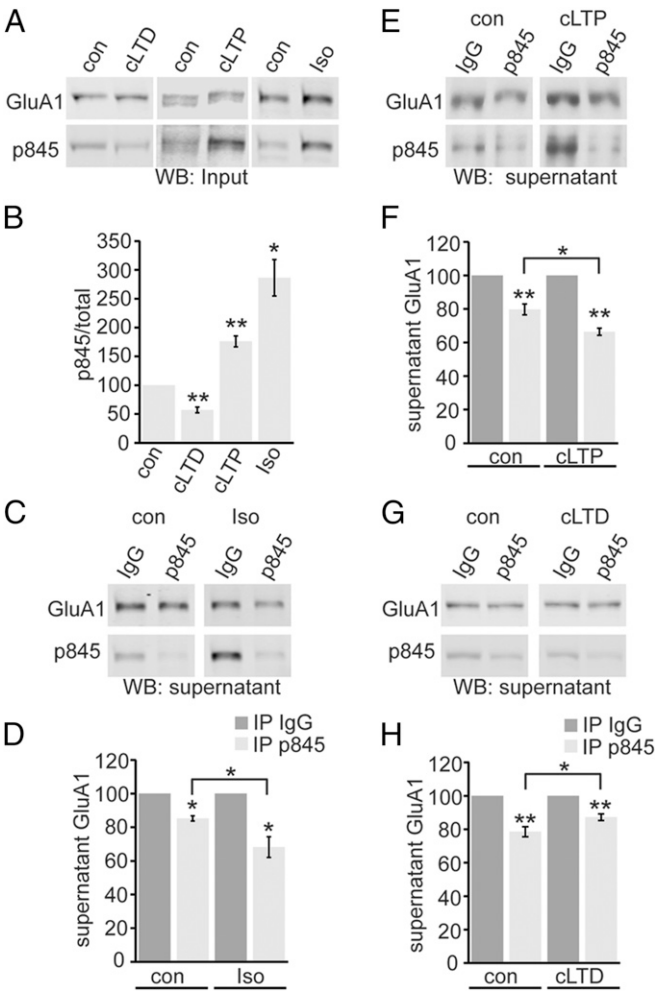

Fig. 3. Changes in phospho-GluA1 S845 during neuronal stimulation. (*A* and *B*) Rat cortical neurons (13–14 DIV) were treated with NMDA-based cLTD, glycine-based cLTP, or Iso. Neurons were lysed and levels of GluA1 phospho-S845 were analyzed by Western blot (*A*) and quantified (*B*). (*C*–*H*) Control, Iso-, cLTP-, or cLTD-treated neuron lysates were subjected to immunodepletion with antiphospho-S845 antibodies. GluA1 remaining in the supernatant was analyzed by Western blot, normalized to control depletion with IgG. Total and phosphorylated GluA1 were detected by Western blot simultaneously using a LiCor fluorescence scanner. (*C* and *D*) Iso-treated neurons, $n = 3$. (*E* and *F*) cLTP-treated neurons, $n = 4$. (*G* and *H*) cLTD-treated neurons, $n = 5$. $^*P < 0.05$ and $^{**}P < 0.01$ indicate significant difference from IgG control. Error bars indicate mean ± SEM.

Quantification of Phospho-GluA1–Containing Receptors in Mouse Forebrain. To examine the levels of GluA1 phosphorylation in vivo, we used our immunodepletion assay to quantify the proportion of GluA1-containing AMPARs phosphorylated at S845 or S831 in mouse forebrain total membrane or synaptic fractions. Adult mice (8–10 wk old) were left in their home cage or exposed to an enriched environment (EE) for 2 h. Forebrains were then dissected and subjected to subcellular fractionation to yield the total membrane (P2) or postsynaptic density fractions (PSD), representing the total or synaptic AMPAR populations, respectively. Two-hour EE exposure greatly increased the levels of the immediate-early genes, Arc (activity-regulated cytoskeleton-associated protein) and Homer1a, in the P2 fraction, indicating that EE exposure activated synaptic plasticity-related gene expression (Fig. S5*A*). EE increased the levels of phospho-S845 and -S831 in the PSD (Fig. 4 *A* and *B*) and P2 (Fig. S5 *B* and *C*).

Immunodepletion under basal conditions showed that 14.2% and 6.3% of GluA1-containing tetramers were phosphorylated at S845 in the P2 or PSD fractions, respectively. EE exposure increased phospho-S845 containing GluA1 tetramers to 19.1% and 22.4% in the P2 and PSD, respectively (Fig. 4 *C*–*F*), whereas 20.5% and 28.5% of GluA1-containing tetramers were phosphorylated at S831 in the P2 and PSD fraction, respectively, under basal conditions, and these proportions increased to 26.1% and 45.6% in the P2 and PSD, respectively, following EE (Fig. 4 *G*–*J*). Again, we find that phospho-S831 is detected in pellets following immunoprecipitation with antiphospho-S845 and vice versa, indicating the presence of GluA1-containing AMPARs bearing phosphorylation at both S845 and S831 in vivo (Fig. S5 *D*–*G*).

The neuromodulator noradrenaline (NA) has been shown to lower the threshold for LTP through activation of PKA and phosphorylation of GluA1 (10, 19). We increased NA levels in mice by intraperitoneal injection of the catecholamine reuptake inhibitor D-amphetamine (2.5 mg/kg). Two hours following injection, we observed a clear increase of phospho-S845 in forebrain P2 fractions compared with vehicle-injected mice. In forebrain P2 fractions, immunodepletion showed that 15.4% and 25.1% of GluA1-containing receptors were phosphorylated at S845 in vehicle or D-amphetamine–injected mice, respectively (Fig. 5). These results show that large populations of GluA1-containing receptors are phosphorylated in vivo, and that these levels show clear increases in behaviorally relevant conditions, such as novel experience or increased levels of neuromodulators.

Specificity of Phospho-GluA1 Antibodies and Characterization of Phospho-GluA1 Using Phos-tag SDS/PAGE. Finally, we examined GluA1 phosphorylation using the Phos-tag SDS/PAGE system described previously (24), in which phosphorylated protein species are separated from unmodified protein through affinity of the phosphate groups with Mn^{2+} ions within the gel (Fig. 6*A*). Phospho-GluA1 species were manipulated by activating PKA or PKC in mouse cortical neurons by FR or PMA treatments, respectively. Antibody specificity was confirmed using neurons cultured from GluA1 S845A or S831A knockin mice. Phospho-S845 signal is absent in GluA1 S845A neurons and phospho-S831 signal is absent in GluA1 S831A neurons. Furthermore, changes in phospho-S845 and S831 occur independently, as the remaining phospho-sites still show sensitivity to FR/PMA treatment in GluA1 knockin neurons (Fig. 6*B*), similar to results obtained from immunostaining (Fig. S1). Using the Phos-tag SDS/PAGE system, significant levels of phosphorylated GluA1 species could be detected as slower migrating bands, which could be positively identified by simultaneous labeling with antiphospho- and total GluA1 (Fig. 6 *C*–*E*). Both phospho-S845 and phospho-S831 appeared as multiple bands under both basal and stimulated conditions, indicating that phosphorylation of GluA1 occurs in multiple combinations, distinct from the faster migrating unphosphorylated

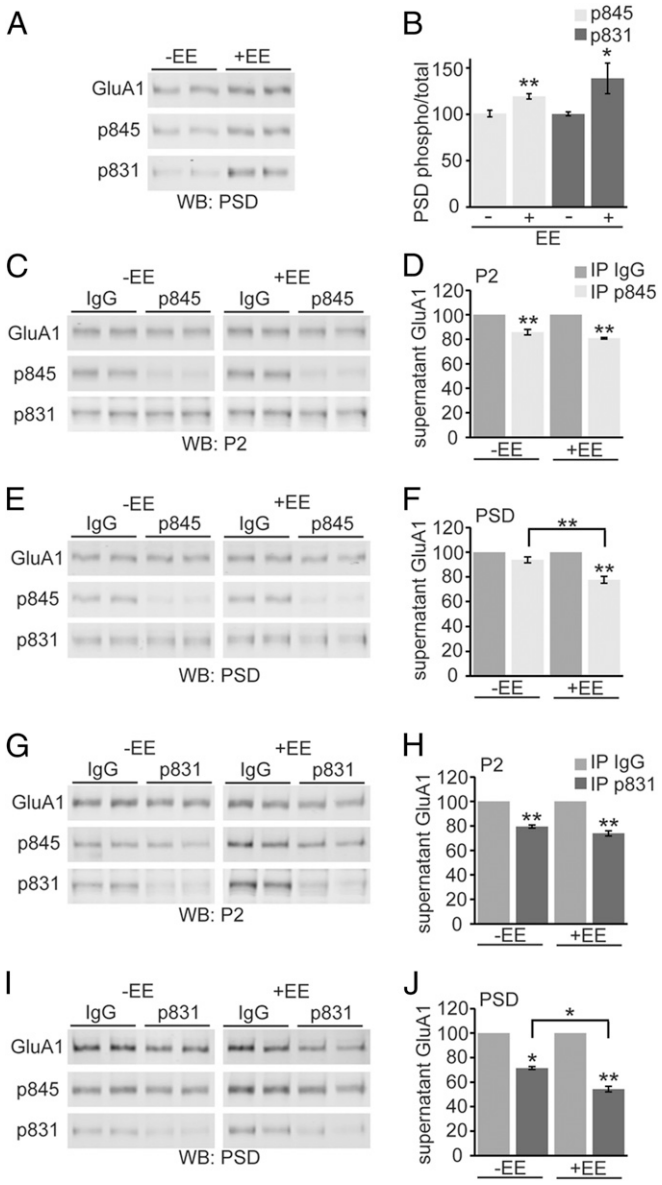

Fig. 4. Exposure to EE increases levels of phospho-GluA1 in adult mouse brain. Male mice (8–10 wk old) were left in their home cage or exposed to an enriched environment (±EE) for 2 h. Forebrains were then dissected and subjected to subcellular fractionation to yield the membrane (P2) or synaptic (PSD) fractions. (*A* and *B*) EE increases the levels of phospho-S845 and phospho-S831 in PSD fractions. $n = 8$. (*C–F*) P2 or PSD lysates were subjected to immunodepletion with antiphospho-S845 antibodies or control IgG. $n = 4$. (*G–J*) P2 or PSD lysates were subjected to immunodepletion with anti-phospho-S831 antibodies. GluA1 remaining in the supernatant following immunodepletion with phospho-specific antibodies was normalized to control depletion with IgG. Total and phosphorylated GluA1 were detected by Western blot simultaneously using a LiCor fluorescence scanner. $n = 4$. $^*P < 0.05$ and $^{**}P < 0.01$ indicate significant difference from IgG control. Error bars indicate mean ± SEM. See also Fig. S5.

GluA1. GluA1 species bearing a single phosphorylation at either S845 or S831 could be unambiguously identified, as these single bands were clearly increased by FR or PMA treatment, respectively (marked by an arrowhead or arrow, respectively, in Fig. 6 *C–E*) and were absent in the respective phospho-deficient mutant neurons. However, a large fraction of phosphorylated (shifted) GluA1 bands, including phospho S845/S831 species, were clearly in a complex population bearing multiple phospho-species, which may represent complex combinations of phospho-GluA1 phosphorylated at S567, S818, S831, T840, S845, and S863 (Fig. 6 *C–E*). It is not clear why we obtained different results from a recent report (24); however, it may be because of difficulty in the quantitative transfer of the phospho-species from the gel to the PVDF membrane using the Phos-tag SDS/PAGE system or improper phosphatase inhibition during and after sample isolation. Finally, because there are at least six known phosphorylation sites on GluA1, which may be phosphorylated independently, there could be 2^6 (or 64) different GluA1 phospho-species, making it extremely difficult to determine stoichiometry at individual sites using the Phos-tag system.

Discussion

Previous work from many laboratories has established a model in which phosphorylation of AMPARs, especially on S845 and S831 of the GluA1 subunit, plays an important role in regulating AMPAR function and synapse targeting during multiple forms of synaptic plasticity, including LTP, LTD, homeostatic scaling, and metaplasticity (1). However, a recent study using a variant Western blot method concluded that basal and stimulated levels of GluA1 phospho-S845 and -S831 were extremely low, calling into question the role of GluA1 phosphorylation in synaptic plasticity (24). Contrary to this recent report, but consistent with many earlier studies, we find that large populations of GluA1-containing AMPARs (20–50%) are phosphorylated under basal and stimulated conditions in vitro and in vivo. We detected the presence of dual-S845/S831 phosphorylated receptors (GluA1 monomers and GluA1-containing tetramers). Furthermore, a recent report (24) predicted, based on their quantification, that only a minority of synapses would contain even a single phosphorylated S845 or S831 GluA1-containing AMPAR. Again in contrast to this recent study, we found that a large fraction of excitatory synapses stain positively for phospho-S845 or -S831 using immunofluorescence microscopy.

Studies using GluA1 and GluA2 phospho-deficient and phospho-mimetic knockin mice have shown that AMPAR phosphorylation is important for several forms of synaptic plasticity and animal behavior. Cortical, hippocampal, and cerebellar LTP/

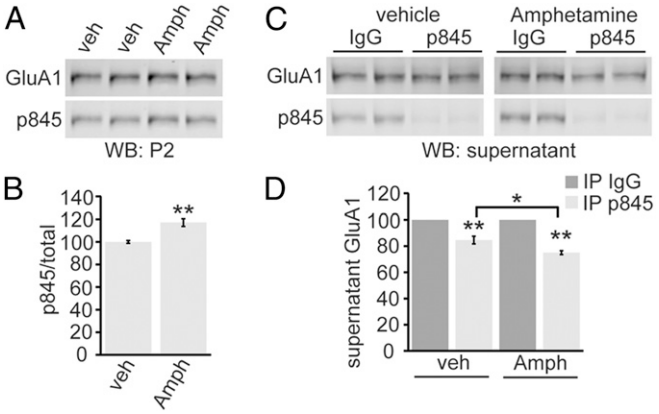

Fig. 5. Amphetamine treatment increased GluA1 phosphorylation in adult mouse brain. Male mice (8 wk old) were injected with vehicle (water) or catecholamine reuptake inhibitor D-amphetamine (2.5 mg/kg). Two-hours post-injection, forebrains were dissected and the membrane (P2) fraction was isolated. P2 lysates were subjected to immunodepletion with antiphospho-S845 antibodies or control IgG. (*A* and *B*) D-amphetamine treatment increases the level of phospho-S845 compared with vehicle injected controls. (*C* and *D*) Phospho-S845 was immunodepleted and GluA1 remaining in the supernatant was quantified, normalized to control immunodepletion with IgG. Total and phosphorylated GluA1 were detected by Western blot simultaneously using a LiCor fluorescence scanner. $n = 6$, $^*P < 0.05$ and $^{**}P < 0.01$ indicate significant difference from IgG control. Error bars indicate mean ± SEM.

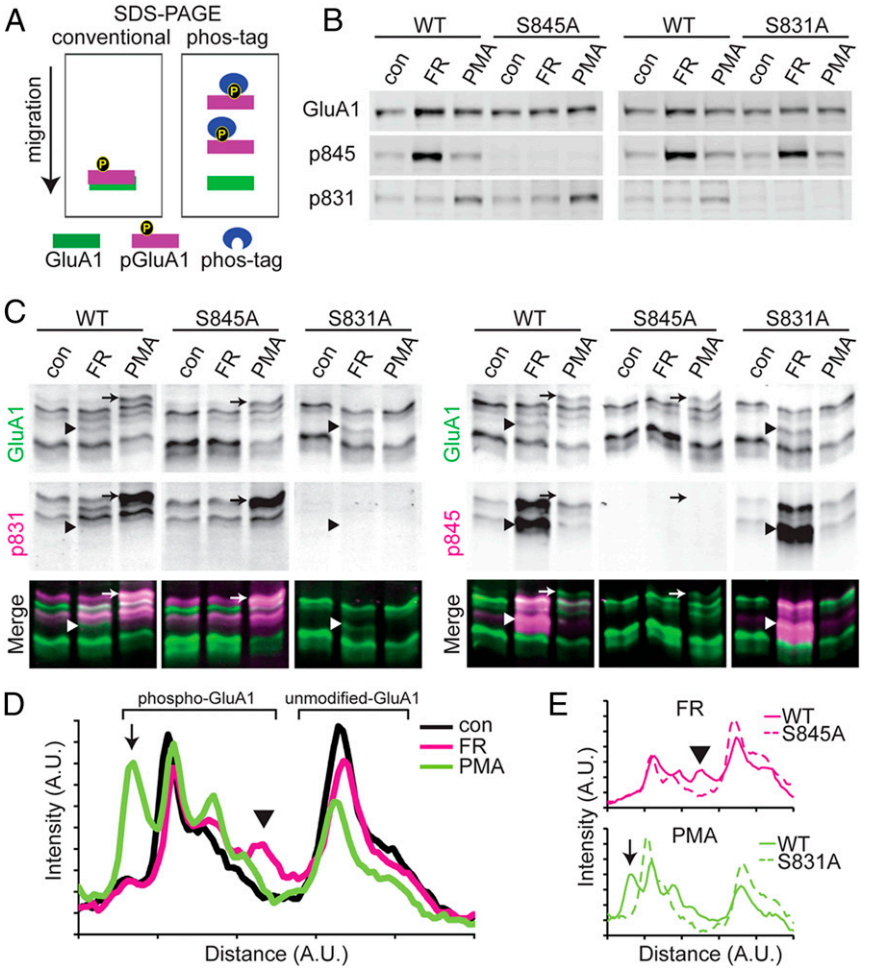

Fig. 6. Detection of phosphorylated GluA1 using Phos-tag SDS/PAGE. (*A*) Schematic of conventional and Phos-tag variant SDS/PAGE. (*B–E*) WT, GluA1 S845A, or GluA1 S831A mutant mouse cortical neurons (14 DIV) were treated with FR or PMA for 10 min. Lysates were subjected to conventional SDS/PAGE (*B*) or Phos-tag SDS/PAGE (*C*). (*D*) Line-scan analysis of Phos-tag Western blot from control and treated WT neurons. Upon stimulation, phosphorylated GluA1 is clearly observed. Singly phosphorylated S845 and S831 are indicated by an arrowhead or arrow, respectively. (*E*) Line scan of Phos-tag Western blot from FR- or PMA-treated WT or mutant neurons. Phospho-GluA1 bands induced by FR or PMA treatment are absent in mutant neurons (arrowhead for phospho-S845 and arrow for phospho-S831). Total and phosphorylated GluA1 were detected by Western blot simultaneously using a LiCor fluorescence scanner.

LTD and hippocampal spatial learning have all been shown to require AMPAR phosphorylation (8, 18, 35). NA modulates the phosphorylation of GluA1 S845, regulates the threshold for LTP induction, and enhances fear-memory formation, and these effects are blocked or occluded by phospho-deficient or phospho-mimetic knockin mice, respectively (10, 19). Moreover, neuromodulators regulate spike timing-dependent synaptic plasticity and this regulation is blocked or occluded by phospho-deficient or phospho-mimetic knockin mice, respectively (10, 19, 23). Fear-memory erasure also requires S845 (21). Serotonin and antidepressants increase phosphorylation of GluA1 S831 and potentiate AMPAR transmission in the temporoammonic pathway with CA1 pyramidal cells, and this potentiation and the effect of antidepressants on stress-induced anhedonia are absent in the S831A knockin mice (20).

In the present study we determined the average levels of S845/S831 phosphorylation in total membrane and PSDs from mouse forebrain. Interestingly, under basal conditions, phospho-S845 receptors were found at higher levels in the total membrane fraction than in the PSD (14.2% in P2 vs. 6.3% in PSD), whereas phospho-S831 receptors were enriched in the PSD (20.5% in P2 vs. 28.5% in PSD). Exploration of the enriched environment increased the levels of phospho-S845 in both the P2 and PSD (19.1% in P2 vs. 22.4% in PSD). These findings are in agreement with earlier work showing that activation of PKA and phosphorylation of S845 promotes the trafficking of GluA1 to the cell surface but that additional signaling (CaMKII activation) is required to recruit these receptors to the PSD (7, 9, 11, 36), and that phosphorylation of GluA1 S845 supports a population of GluA1-containing receptors localized to peri-synaptic regions (37). Thus, in agreement with earlier work, or data suggest that phospho-S845 receptors may accumulate at extrasynaptic sites under basal conditions and coordinated activation of multiple signaling pathways (PKA and CaMKII) can recruit these phospho-S845 receptors to synapses contributing to synaptic potentiation.

GluA1-containing AMPAR tetramers could be phosphorylated at S845/S831 to different degrees of saturation, two sites for heteromeric receptors and four sites for GluA1 homomers. Phosphorylation of S845/S831 can modify single-channel properties (5, 14, 15), but also plays a clear role in receptor trafficking and synapse retention (1). It is not known whether phosphorylation of S845 and S831 on the same or separate subunits within tetramers to varying degrees of saturation may act cooperatively to regulate receptor trafficking/channel properties of the intact tetramer. In cultured cortical neurons at basal states, we find that ~20% of GluA1-containing tetramers are phosphorylated at S845 or S831, whereas under full-denaturing conditions we find that

~10% of GluA1 monomers are phosphorylated, confirming that many AMPAR tetramers are only partially phosphorylated. Neuronal stimulation may increase the saturation of a particular phospho-site or increase the population-bearing phosphorylations at different sites. In our Phos-tag experiments we are able to detect single phosphorylated S845 or S831 species, as well as a more complex population-containing multiple phosphorylations. GluA1 is also known to be phosphorylated at S567 by CaMKII (38), S818 and T840 by PKC (39, 40), and more recently at S863 by PAK3 (41). Interestingly, we recently showed that stimulation of neurons with the neuropeptide PACAP38 resulted in coordinated increases in phosphorylation of GluA1 S845 and dephosphorylation of T840 (42), indicating a complex relationship exists between different phosphorylation sites. The extent to which phosphorylation of different sites (S845 and S831) or of the same site on separate monomers act in coordination will likely be a complex and important question to address in future studies. As mentioned in *Results*, because there are at least six known phosphorylation sites on GluA1 that may be phosphorylated independently, there could be 2^6 (or 64) different GluA1 phospho-species, making it extremely difficult to determine stoichiometry at individual sites using the Phos-tag system. Furthermore, it is interesting to note that phosphorylation may act synergistically with other posttranslational modifications, such as palmitoylation (43), S-nitrosylation (44), and ubiquitination (25).

Finally, it is important to note that in chemically isolated dendritic spines, synaptic plasticity and AMPAR phosphorylation can occur in a highly localized fashion. Spines separated by microns may even show opposite changes. Our present study and previous work (24) can only make conclusions regarding the average stoichiometry of receptor modification within the cell or subcellular fraction. AMPAR phosphorylation could occur to far greater or lesser extents within individual synapses with important functional consequences.

In conclusion, phosphorylated species of GluA1 are abundant, wide-spread, and are highly responsive to numerous physiologically relevant stimuli. This characterization reaffirms a large body of work showing a prominent role of AMPAR phosphorylation in controlling AMPAR trafficking and synaptic plasticity.

Materials and Methods

Animal Use and EE. All animals were treated in accordance with the Johns Hopkins University Animal Care and Use Committee guidelines. For all experiments, mice were 8- to 10-wk old. Mice were either left in their home cage or allowed to explore an enriched environment for 2 h (a large cage containing novel objects, tubes, and strings of beads suspended from the cage lid). Mice were then anesthetized by inhalation of isoflurane for 15 s, followed immediately by cervical dislocation, brains were removed, and forebrains (cerebral cortex and hippocampus) were dissected in ice-cold PBS and immediately frozen on dry ice. Samples were kept at −80 °C until used for subcellular fractionation.

Amphetamine Treatment. Mice were treated by intraperitoneal injection with vehicle (water) or D-amphetamine (2.5 mg/kg). Two hours postinjection, mice were killed and brains were prepared as described above.

Neuron Culture and Drug Treatment. Cortical neurons obtained from Sprague–Dawley rats or C57BL/6 mice at embryonic day 18 were plated onto poly-L-lysine–coated tissue culture dishes or glass coverslips and grown in glia-conditioned neurobasal media (Invitrogen) supplemented with 2% (vol/vol) B-27, 2 mM Glutamax, 50 U/mL PenStrep, and 1% horse serum (Invitrogen). Cultured cortical neurons were fed twice per week. For all experiments cortical neurons (grown for 13–14 d in vitro, DIV) were plated at a density of 600,000 cells per well into standard 6-well tissue culture plates or 250,000 cells per well into 12-well tissue culture plates. In some experiments cortical neurons were treated with FR (5 μM/100 nM), PMA (1 μM), or Iso (5 μM) for 10 min, as indicated (drugs added to the culture media). For cLTD, neurons were incubated in artificial cerebrospinal fluid (ACSF) (143 mM NaCl, 5 mM KCl, 10 mM Hepes pH 7.4, 10 mM glucose, 2 mM $CaCl_2$, 1 mM $MgCl_2$) for 30 min followed by ACSF containing NMDA 40 μM for 3 min. For cLTP, neurons were pretreated for 30 min in ACSF, treated for 5 min with Mg^{2+}-free ACSF containing 200 μM glycine, and then returned to Mg^{2+}-containing ACSF without glycine for 20 min before lysis. All incubation steps for cLTP contained 0.5 μM tetrodotoxin, 20 μM bicuculline, and 1 μM strychnine. Hippocampal neurons were obtained from Sprague–Dawley rates at embryonic day 18, plated onto poly-L-lysine–coated glass coverslips, and grown in neurobasal media (Invitrogen) supplemented with 2% (vol/vol) B27 (Invitrogen), 0.5 mM glutamine, and 12.5 μM glutamate, 50 U/mL PenStrep (Gibco).

Antibodies. The following mouse monoclonal primary antibodies were used: anti-GluA1 N-terminal antibody (4.9D, made in house), anti-Arc (made in house), and antitubulin (Sigma). The following rabbit primary antibodies were used: anti-GluA1 phospho-S845 specific and antiphospho-S831 specific (Millipore), and Homer1a (Synaptic Systems). The following additional antibodies were used: guinea pig anti-vGlut1 (SynapticSystems); IRDye650-conjugated goat anti-mouse and IRDye800-conjugated goat anti-rabbit (Li-Cor); horseradish peroxidase-conjugated anti-rabbit and anti-mouse (Thermo Fisher Scientific); horseradish peroxidase-conjugated goat anti-mouse and mouse anti-rabbit light-chain specific (Jackson Laboratories); and Alexa Fluor (Invitrogen) conjugates 568 goat anti-rabbit, 488 goat anti-mouse, 647 goat anti-guinea pig.

Immunofluorescence Microscopy. Hippocampal neurons fixed in 4% (vol/vol) paraformaldehyde/4% (wt/vol) sucrose for 3 min, followed by 90-s immersion in ice-cold methanol, were washed in PBS before incubation with primary antibodies overnight at 4 °C in 1× GDB buffer (30 mM phosphate buffer, pH 7.4, containing 0.2% gelatin, 0.5% Triton X-100, and 0.8 M NaCl), followed by secondary antibodies for 2–4 h in GDB buffer. For some experiments, fixed hippocampal neurons were treated with alkaline phosphatase for 4 h before immunostaining. An LSM510 confocal microscope system (Zeiss) was used to acquire fixed neuron *z*-series image stacks that encompassed entire dendrite segments and maximum-projected into a single slice and analyzed using Fiji ImageJ software. For integrated intensity quantification, immunostained channels were parsed into separate images for at least 10 neurons per condition, and a threshold level for each channel was set manually to exclude diffuse background staining and cell bodies. To quantify the synaptic phospho-AMPAR, immunofluorescence images were maximum-projected into a single slice and smoothed using a Gaussian filter. Threshold levels for vGlut1 and total GluA1 channel were set manually to exclude diffuse background staining. The average phospho-AMPAR signal intensity was analyzed within regions qualified as synapses. Synapses were defined as thresholded puncta that were positive for both vGlut1 and total GluA1 immunostaining. A size filter was applied to remove background noise and cell bodies. To quantify the percentage of phospho-AMPAR$^+$ synapses, the frequency distribution of the average phospho-AMPAR signal intensity was plotted and the thresholds were set as two SDs higher than the mean of the control group, with 4-h CIP treatment. Synapses with phospho-AMPAR signal intensity above threshold were counted as positive, with a limited 3% margin of error. Identical settings were applied to each image acquired within an experiment.

Phospho-AMPAR Immunodepletion. Following experimental treatment, neurons were lysed in lysis buffer [1% Triton X-100, 0.5% sodium deoxycholate, 0.02% SDS, 50 mM NaF, 5 mM sodium pyrophosphate, 1 mM EDTA, 200 nM okadaic acid, protease inhibitor mixture (Roche), in PBS]. Lysates were cleared by centrifugation at 17,000 × *g* at 4 °C for 20 min. In some experiments cells were lysed without phosphatase inhibitors and lysates were treated with shrimp alkaline phosphatase (Roche) in the presence of 10 mM $MgCl_2$ at 37 °C overnight. Lysates were subjected to immunodepletion by addition of rabbit control IgG, antiphospho-S845 or antiphospho-S831 (5 μg/mL, each) together with 20 μL of protein A Sepharose beads (GE Healthcare), followed by agitation overnight at 4 °C. Sepharose beads were pelleted by centrifugation at 500 × *g* at 4 °C. The supernatant was collected and subjected to SDS/PAGE and Western blot. The remaining beads were washed thoroughly with lysis buffer, proteins were eluted using SDS-sample buffer, and eluates were analyzed by SDS/PAGE and Western blot. The immunoreactive phospho- and total GluA1 signals were detected simultaneously with a Li-Cor Odyssey CLx IR imaging system (Li-Cor). Alternatively, for maximal denaturation, cells were collected by scraping in homogenization buffer, pelleted by centrifugation at 500 × *g*, and then lysed in prewarmed SDS-buffer [1% SDS, 50 mM NaF, 5 mM sodium pyrophosphate, 1 mM EDTA, 200 nM okadaic acid, protease inhibitor mixture (Roche), in PBS]. Lysates were incubated for 20 min at 37 °C, and then diluted 10 times with Triton X-100 buffer [1% TX-100, 50 mM NaF, 5 mM sodium pyrophosphate, 1 mM EDTA, 200 nM okadaic acid, protease inhibitor mixture (Roche), in PBS], and incubated for a

further 20 min at 4 °C with agitation. Lysates were then cleared by centrifugation and subjected to immunodepletion, as described above.

PSD Preparation. Frozen forebrains were homogenized using 12 strokes from a glass homogenizer in ice-cold homogenization solution [320 mM sucrose, 10 mM Hepes pH 7.4, 1 mM EDTA, 5 mM Na pyrophosphate, 200 nM okadaic acid, protease inhibitor mixture (Roche)]. Brain homogenate was then centrifuged at 800 × *g* for 10 min at 4 °C to obtain the P1 and S1 fractions. The S1 fraction was then subjected to centrifugation at 16,000 × *g* for 20 min at 4 °C to obtain the P2 and S2 fractions. The P2 fraction was resuspended in homogenization buffer, layered on top of a discontinuous sucrose density gradient [0.8 M, 1.0 M, or 1.2 M sucrose in 10 mM Hepes pH 7.4, 1 mM EDTA, 5 mM Na pyrophosphate, 200 nM okadaic acid, protease inhibitor mixture (Roche)], and then subjected to ultracentrifugation at 82,500 × *g* for 2 h at 4 °C. Material accumulated at the interface of 1.0 M and 1.2 M sucrose (synaptosomes) was collected. Synaptosomes were diluted using 10 mM Hepes pH 7.4 (containing protease and phosphatase inhibitors) to restore the sucrose concentration back to 320 mM. The diluted synaptosomes were then pelleted by centrifugation at 100,000 × *g* for 30 min at 4 °C. The synaptosome pellet was then resuspended in 50 mM Hepes pH 7.4 and then mixed with an equal part 1% Triton X-100 (both solutions contained protease and phosphatase inhibitors). This mixture was incubated at 4 °C with rotation for 15 min followed by centrifugation at 32,000 × *g* for 20 min to yield the PSD preparation. P2 or PSD fractions were resuspended/lysed using lysis buffer, protein concentration was quantified using Bradford assay, and lysates were subjected to immunodepletion with control rabbit IgG or antiphospho-S845 and antiphospho-S831 antibodies, as described above.

Phos-tag Western Blot. For Phos-tag Western blot, 5% acrylamide gel was mixed with 50 μM Phos-tag acrylamide (AAL-107, Wako) and 100 μM $MnCl_2$. After sample separation on Mn^{2+}-Phos-tag SDS/PAGE gel, the gel was washed with transfer buffer containing 1 mM EDTA for 10 min, with gentle agitation to eliminate Mn^{2+} ions from the gel, followed by washing with normal transfer buffer without EDTA for another 10 min. Proteins were transferred to PVDF membrane using a wet-tank method and used for Western blotting using monoclonal antiphospho-GluA1 S831, monoclonal antiphospho-GluA1 S845, and total GluA1 antibodies. The immunoreactive phospho- and total GluA1 signals were detected simultaneously with a Li-Cor Odyssey CLx IR imaging system (Li-Cor).

Statistics. Pair-wise comparisons were performed using an unpaired, two-tailed Student's *t* test. Multiple comparisons were performed using one-way ANOVA with Fisher's PLSD post hoc test. Statistical significance was considered as $P < 0.05$.

ACKNOWLEDGMENTS. We thank members of the R.L.H. laboratory for helpful discussion, especially Dr. Ingie Hong. This work was supported by grants from the National Institute of Health, the Howard Hughes Medical Institute (to R.L.H.), and the Canadian Institute for Health Research (to G.H.D.).

1. Huganir RL, Nicoll RA (2013) AMPARs and synaptic plasticity: The last 25 years. *Neuron* 80(3):704–717.
2. Roche KW, O'Brien RJ, Mammen AL, Bernhardt J, Huganir RL (1996) Characterization of multiple phosphorylation sites on the AMPA receptor GluR1 subunit. *Neuron* 16(6):1179–1188.
3. Mammen AL, Kameyama K, Roche KW, Huganir RL (1997) Phosphorylation of the alpha-amino-3-hydroxy-5-methylisoxazole4-propionic acid receptor GluR1 subunit by calcium/calmodulin-dependent kinase II. *J Biol Chem* 272(51):32528–32533.
4. Barria A, Derkach V, Soderling T (1997) Identification of the Ca2+/calmodulin-dependent protein kinase II regulatory phosphorylation site in the alpha-amino-3-hydroxyl-5-methyl-4-isoxazole-propionate-type glutamate receptor. *J Biol Chem* 272(52):32727–32730.
5. Banke TG, et al. (2000) Control of GluR1 AMPA receptor function by cAMP-dependent protein kinase. *J Neurosci* 20(1):89–102.
6. Ehlers MD (2000) Reinsertion or degradation of AMPA receptors determined by activity-dependent endocytic sorting. *Neuron* 28(2):511–525.
7. Esteban JA, et al. (2003) PKA phosphorylation of AMPA receptor subunits controls synaptic trafficking underlying plasticity. *Nat Neurosci* 6(2):136–143.
8. Lee HK, et al. (2003) Phosphorylation of the AMPA receptor GluR1 subunit is required for synaptic plasticity and retention of spatial memory. *Cell* 112(5):631–643.
9. Oh MC, Derkach VA, Guire ES, Soderling TR (2006) Extrasynaptic membrane trafficking regulated by GluR1 serine 845 phosphorylation primes AMPA receptors for long-term potentiation. *J Biol Chem* 281(2):752–758.
10. Man HY, Sekine-Aizawa Y, Huganir RL (2007) Regulation of alpha-amino-3-hydroxy-5-methyl-4-isoxazolepropionic acid receptor trafficking through PKA phosphorylation of the Glu receptor 1 subunit. *Proc Natl Acad Sci USA* 104(9):3579–3584.
11. Diering GH, Gustina AS, Huganir RL (2014) PKA-GluA1 coupling via AKAP5 controls AMPA receptor phosphorylation and cell-surface targeting during bidirectional homeostatic plasticity. *Neuron* 84(4):790–805.
12. Kim S, Ziff EB (2014) Calcineurin mediates synaptic scaling via synaptic trafficking of Ca2+-permeable AMPA receptors. *PLoS Biol* 12(7):e1001900.
13. Lee HK, Barbarosie M, Kameyama K, Bear MF, Huganir RL (2000) Regulation of distinct AMPA receptor phosphorylation sites during bidirectional synaptic plasticity. *Nature* 405(6789):955–959.
14. Derkach V, Barria A, Soderling TR (1999) Ca2+/calmodulin-kinase II enhances channel conductance of alpha-amino-3-hydroxy-5-methyl-4-isoxazolepropionate type glutamate receptors. *Proc Natl Acad Sci USA* 96(6):3269–3274.
15. Kristensen AS, et al. (2011) Mechanism of Ca2+/calmodulin-dependent kinase II regulation of AMPA receptor gating. *Nat Neurosci* 14(6):727–735.
16. Barria A, Muller D, Derkach V, Griffith LC, Soderling TR (1997) Regulatory phosphorylation of AMPA-type glutamate receptors by CaM-KII during long-term potentiation. *Science* 276(5321):2042–2045.
17. Goel A, et al. (2011) Phosphorylation of AMPA receptors is required for sensory deprivation-induced homeostatic synaptic plasticity. *PLoS One* 6(3):e18264.
18. Huang S, et al. (2012) Pull-push neuromodulation of LTP and LTD enables bidirectional experience-induced synaptic scaling in visual cortex. *Neuron* 73(3):497–510.
19. Makino Y, Johnson RC, Yu Y, Takamiya K, Huganir RL (2011) Enhanced synaptic plasticity in mice with phosphomimetic mutation of the GluA1 AMPA receptor. *Proc Natl Acad Sci USA* 108(20):8450–8455.
20. Cai X, et al. (2013) Local potentiation of excitatory synapses by serotonin and its alteration in rodent models of depression. *Nat Neurosci* 16(4):464–472.
21. Clem RL, Huganir RL (2010) Calcium-permeable AMPA receptor dynamics mediate fear memory erasure. *Science* 330(6007):1108–1112.
22. Crombag HS, et al. (2008) A necessary role for GluR1 serine 831 phosphorylation in appetitive incentive learning. *Behav Brain Res* 191(2):178–183.
23. Seol GH, et al. (2007) Neuromodulators control the polarity of spike-timing-dependent synaptic plasticity. *Neuron* 55(6):919–929.
24. Hosokawa T, Mitsushima D, Kaneko R, Hayashi Y (2015) Stoichiometry and phosphoisotypes of hippocampal AMPA-type glutamate receptor phosphorylation. *Neuron* 85(1):60–67.
25. Widagdo J, et al. (2015) Activity-dependent ubiquitination of GluA1 and GluA2 regulates AMPA receptor intracellular sorting and degradation. *Cell Rep* 10(5):783–795.
26. Lu W, et al. (2001) Activation of synaptic NMDA receptors induces membrane insertion of new AMPA receptors and LTP in cultured hippocampal neurons. *Neuron* 29(1):243–254.
27. Lee HK, Kameyama K, Huganir RL, Bear MF (1998) NMDA induces long-term synaptic depression and dephosphorylation of the GluR1 subunit of AMPA receptors in hippocampus. *Neuron* 21(5):1151–1162.
28. Liao D, Scannevin RH, Huganir R (2001) Activation of silent synapses by rapid activity-dependent synaptic recruitment of AMPA receptors. *J Neurosci* 21(16):6008–6017.
29. He K, Goel A, Ciarkowski CE, Song L, Lee HK (2011) Brain area specific regulation of synaptic AMPA receptors by phosphorylation. *Commun Integr Biol* 4(5):569–572.
30. Tenorio G, et al. (2010) 'Silent' priming of translation-dependent LTP by ß-adrenergic receptors involves phosphorylation and recruitment of AMPA receptors. *Learn Mem* 17(12):627–638.
31. Lee HK, Takamiya K, He K, Song L, Huganir RL (2010) Specific roles of AMPA receptor subunit GluR1 (GluA1) phosphorylation sites in regulating synaptic plasticity in the CA1 region of hippocampus. *J Neurophysiol* 103(1):479–489.
32. Ai H, et al. (2011) Differential regulation of AMPA receptor GluA1 phosphorylation at serine 831 and 845 associated with activation of NMDA receptor subpopulations. *Neurosci Lett* 497(2):94–98.
33. Davies KD, Goebel-Goody SM, Coultrap SJ, Browning MD (2008) Long term synaptic depression that is associated with GluR1 dephosphorylation but not alpha-amino-3-hydroxy-5-methyl-4-isoxazolepropionic acid (AMPA) receptor internalization. *J Biol Chem* 283(48):33138–33146.
34. Bevilaqua LR, Medina JH, Izquierdo I, Cammarota M (2005) Memory consolidation induces N-methyl-D-aspartic acid-receptor- and Ca2+/calmodulin-dependent protein kinase II-dependent modifications in alpha-amino-3-hydroxy-5-methylisoxazole-4-propionic acid receptor properties. *Neuroscience* 136(2):397–403.
35. Steinberg JP, et al. (2006) Targeted in vivo mutations of the AMPA receptor subunit GluR2 and its interacting protein PICK1 eliminate cerebellar long-term depression. *Neuron* 49(6):845–860.
36. Sun X, Zhao Y, Wolf ME (2005) Dopamine receptor stimulation modulates AMPA receptor synaptic insertion in prefrontal cortex neurons. *J Neurosci* 25(32):7342–7351.
37. He K, et al. (2009) Stabilization of Ca2+-permeable AMPA receptors at perisynaptic sites by GluR1-S845 phosphorylation. *Proc Natl Acad Sci USA* 106(47):20033–20038.
38. Lu W, Isozaki K, Roche KW, Nicoll RA (2010) Synaptic targeting of AMPA receptors is regulated by a CaMKII site in the first intracellular loop of GluA1. *Proc Natl Acad Sci USA* 107(51):22266–22271.
39. Boehm J, et al. (2006) Synaptic incorporation of AMPA receptors during LTP is controlled by a PKC phosphorylation site on GluR1. *Neuron* 51(2):213–225.
40. Lee HK, et al. (2007) Identification and characterization of a novel phosphorylation site on the GluR1 subunit of AMPA receptors. *Mol Cell Neurosci* 36(1):86–94.
41. Hussain NK, Thomas GM, Luo J, Huganir RL (2015) Regulation of AMPA receptor subunit GluA1 surface expression by PAK3 phosphorylation. *Proc Natl Acad Sci USA* 112(43):E5883–E5890.
42. Toda AM, Huganir RL (2015) Regulation of AMPA receptor phosphorylation by the neuropeptide PACAP38. *Proc Natl Acad Sci USA* 112(21):6712–6717.
43. Lin DT, et al. (2009) Regulation of AMPA receptor extrasynaptic insertion by 4.1N, phosphorylation and palmitoylation. *Nat Neurosci* 12(7):879–887.
44. Selvakumar B, et al. (2013) S-nitrosylation of AMPA receptor GluA1 regulates phosphorylation, single-channel conductance, and endocytosis. *Proc Natl Acad Sci USA* 110(3):1077–1082.

Supporting Information

Diering et al. 10.1073/pnas.1610631113

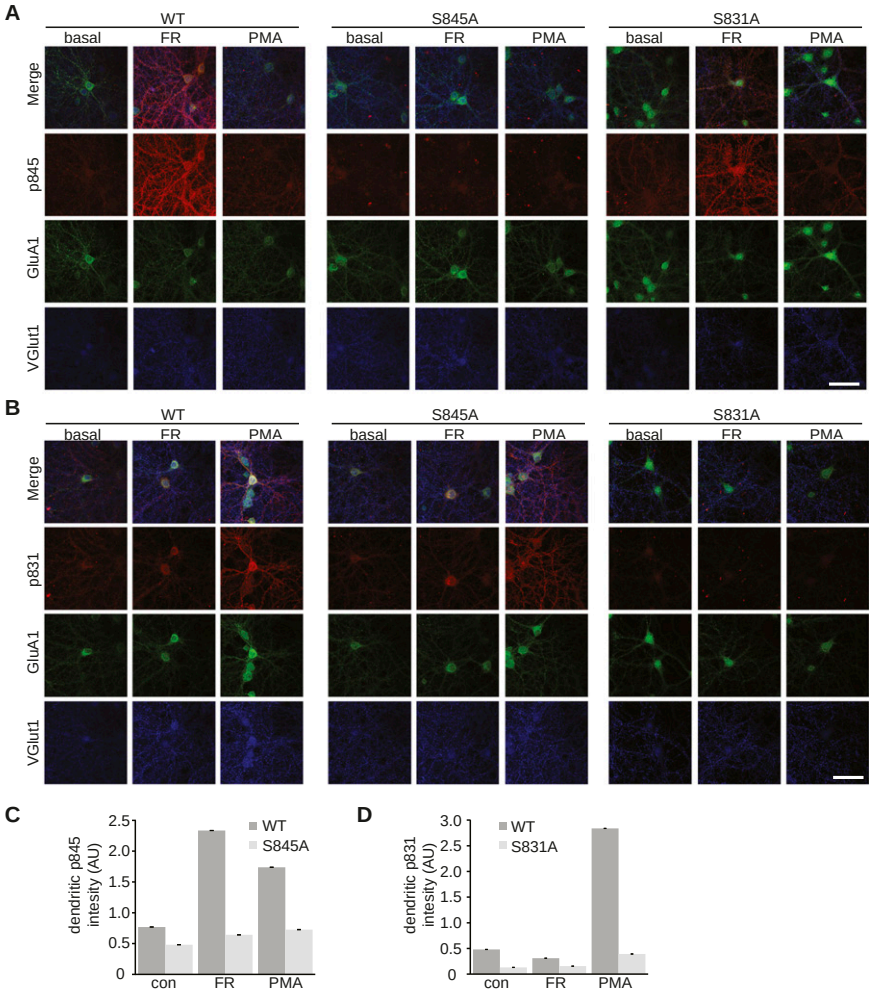

Fig. S1. Confirmation of phospho-S845 and phospho-S831 staining specificity. (*A* and *B*) WT, GluA1 S845A, or -S831A knockin mouse cortical neurons (14–15 DIV) were treated with FR or PMA for 10 min followed by fixation and immunolabeling. (Scale bars, 50 μm.) FR treatment greatly increases the staining intensity of antiphospho-S845 in WT and S831A neurons but not in S845A neurons. PMA treatment greatly increases the staining intensity of antiphospho-S831 in WT and S845A neurons but not S831A neurons. (*C* and *D*) Quantification of staining intensity of antiphospho-S845 or S831. $n = 7–12$ cells per condition. Error bars indicate mean ± SEM.

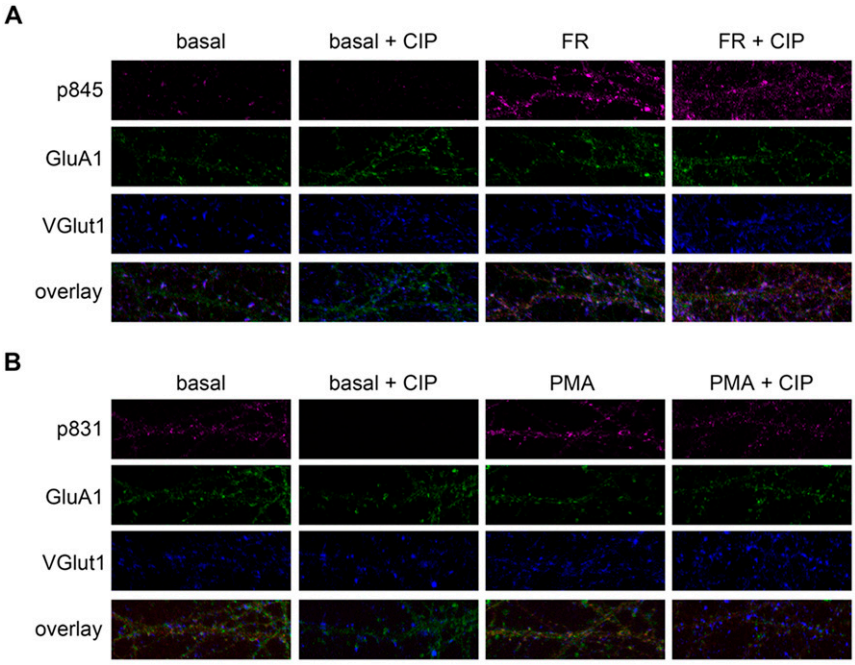

Fig. S2. Phosphatase treatment and immunofluorescence detection of synaptic phospho-S845 and -S831. Rat hippocampal neurons (14 DIV) were left untreated (basal) or treated with FR or PMA for 10 min, followed by fixation, and phosphatase treatment for 4 h, as indicated (CIP) before immunolabeling. Representative images of 50-μm dendritic segments immunostained with phospho-S845 (*A*) or phospho-S831 (*B*) show synaptic localization (defined as immunostaining that overlaps with both total GluA1 and the excitatory synapse marker VGlut1), which was greatly increased upon FR or PMA treatment, respectively, and greatly reduced upon phosphatase treatments.

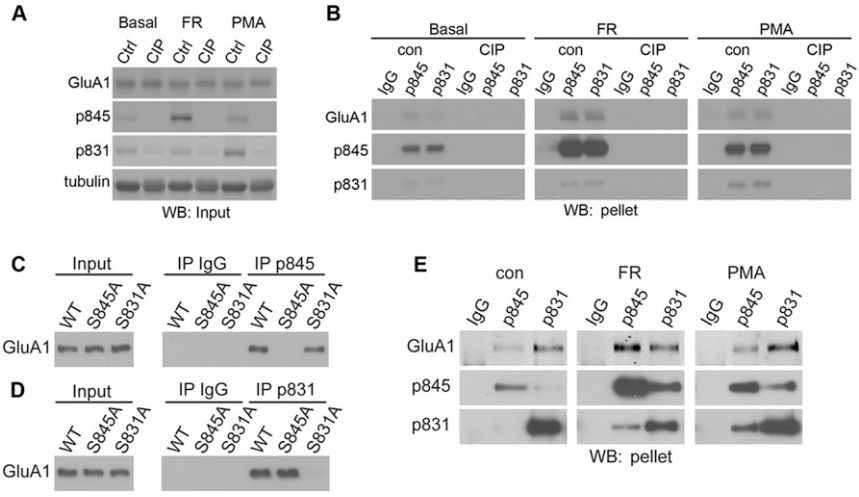

Fig. S3. Immunoprecipitation of phospho-GluA1 containing tetramers. (*A* and *B*) WT rat cortical neurons (14 DIV) were treated with FR or PMA for 10 min before lysis. Lysates were treated with or without alkaline phosphatase and subjected to immunoprecipitation with antiphospho-S845 or phospho-S831 antibodies. (*A*) Alkaline phosphatase can dephosphorylate phospho-S845 and phospho-S831 under basal and stimulated conditions, but the total GluA1 level was not changed. (*B*) Antiphospho-S845 or antiphospho-S831 antibodies can immunoprecipitate GluA1 from control lysates but not from phosphatase-treated lysates, indicating the specific immunoprecipitation of phosphorylated GluA1 with anti-pS845 and pS831 antibodies. (*C* and *D*) WT, GluA1 S845A, or GluA1 S831A mutant mouse cortical neurons (14 DIV) were treated with FR (*C*) or PMA (*D*) for 10 min before lysis and immunoprecipitation with antiphospho-S845 or phospho-S831. (*C*) Antiphospho-S845 can immunoprecipitate GluA1 from WT and S831A but not from S845A phospho-mutant lysates. (*D*) Antiphospho-S831 can immunoprecipitate GluA1 from WT and S845A but not from S831A phospho-mutant lysates. (*E*) In FR/PMA-treated neuron lysates, phospho-S831 can be detected following immunoprecipitation of phospho-S845 and vice versa, indicating the presence of dual phospho-S845/phospho-S831 containing GluA1 tetramers.

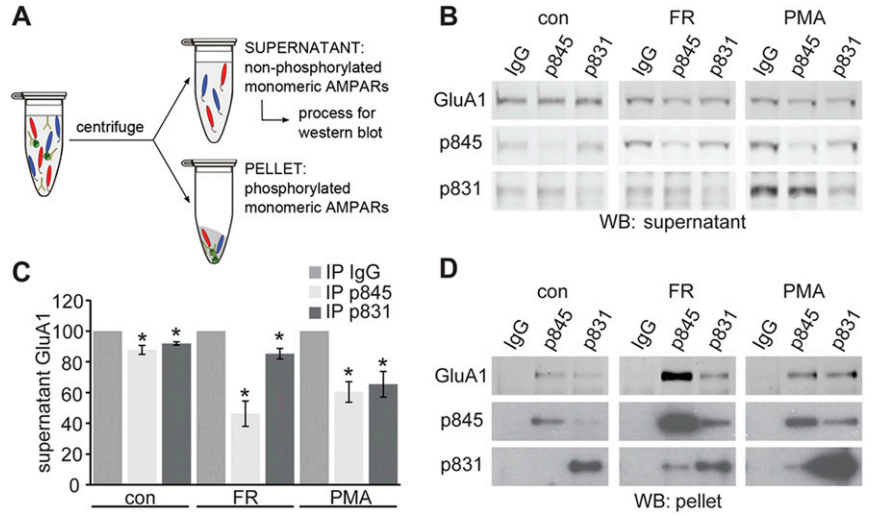

Fig. S4. Immunoprecipitation of phosphorylated GluA1 monomers. (*A*) Schematic immunoprecipitation of phosphorylated GluA1 under maximal denaturation conditions (monomers). (*B–D*) Rat cortical neurons (13–14 DIV) were treated with FR or PMA for 10 min. Neurons were then lysed under maximal denaturation conditions to separate AMPAR tetramers into monomers. (*B*) Maximum-denaturation neuronal lysates were subjected to immunodepletion with antiphospho-S845 or antiphospho-S831 antibodies, followed by Western blot of the supernatant. (*C*) Quantification of GluA1 remaining in the supernatant following immunodepletion, normalized to control immunodepletion with IgG. $n = 3$; $^*P < 0.05$ indicates significant difference from IgG control. (*D*) Western blot analysis of the eluate (pellet) following immunodepletion. In treated neurons, phospho-S831 can be detected following immunoprecipitation of phospho-S845 and vice versa, indicating the presence of dual phospho-S845/phospho-S831 containing GluA1 monomers. $^*P < 0.05$. Error bars indicate mean ± SEM.

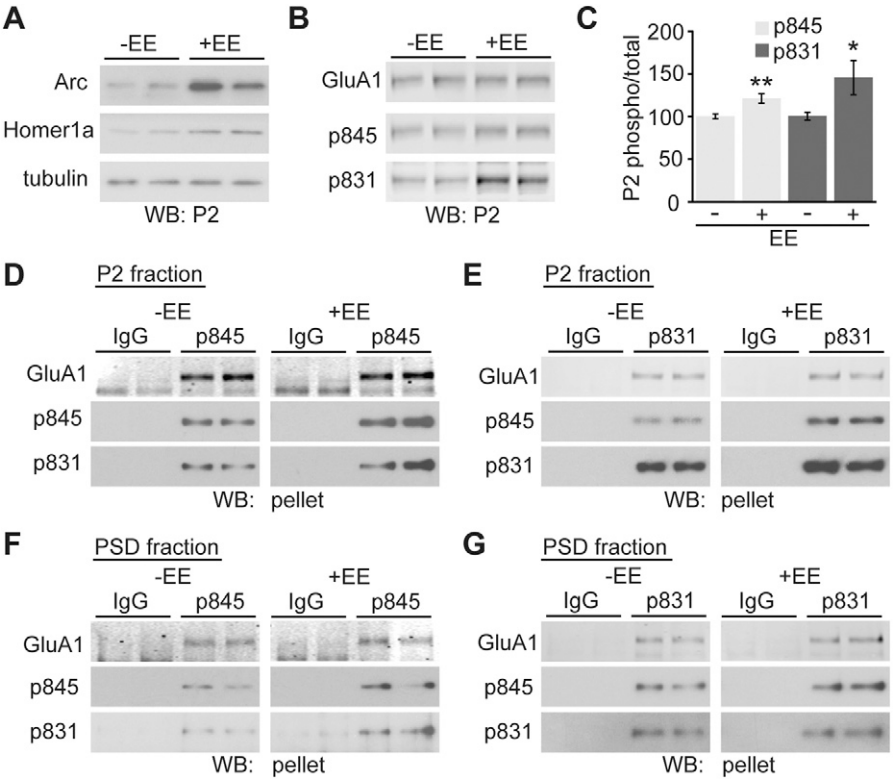

Fig. S5. EE affects GluA1 phosphorylation. Male mice (8–10 wk old) were left in their home cage or exposed to an enriched environment (±EE) for 2 h. Forebrains were then dissected and subjected to subcellular fractionation to yield the membrane (P2) or synaptic (PSD) fractions. (*A*) Two-hour EE exposure increases the expression of immediate-early genes Arc and Homer1a in P2 fraction. (*B* and *C*) EE increases the levels phospho-S845 and phospho-S831 in P2 fractions. $n = 8$. $^*P < 0.05$ and $^{**}P < 0.01$. Error bars indicate mean ± SEM (*D–G*) Western blot analysis of the eluate following immunodepletion. In mouse P2 or PSD lysates, phospho-S831 can be detected following immunoprecipitation of phospho-S845 and vice versa, indicating the presence of dual phospho-S845/phospho-S831 containing GluA1 tetramers.